Biochimica et Biophysica Acta, 1059 (1991) 312–322

ADONIS 000527289100207G

BBABIO 43466

Characteristics of two atrazine-binding sites that specifically inhibit Photosystem II function

Paul A. Jursinic [1], Susan A. McCarthy [1], Terry M. Bricker [2] and Alan Stemler [3]

[1] *Plant Biochemistry Research, Northern Regional Research Center, Agricultural Research Service, U.S. Department of Agriculture, IL (U.S.A.),* [2] *Department of Botany and Biochemistry, Louisiana State University, Baton Route, LA (U.S.A.) and* [3] *Botany Department, University of California, Davis, CA (U.S.A.)*

(Received 27 December 1990)
(Revised manuscript received 17 May 1991)

Key words: Atrazine; Herbicide; Charge recombination; Unspecific binding; Photoaffinity labelling; Photosystem II concentration

In pea thylakoids, [^{14}C]atrazine is found to have two binding sites per active oxygen-evolving complex; one with high-binding affinity and one with low-binding affinity. The high affinity site has a K_d = 80 nM, is present at a concentration of 120 nM (1 site/470 Chl); binds in less than 500 ms; and blocks the electron flow reaction, $Q_a^- Q_b \rightarrow Q_a Q_b^-$. The low affinity site has a K_d = 420 nM; is present at a concentration of 120 nM (1 site/470 Chl); binds with a half-time of 4 to 5 s; and partially inhibits the charge recombination reaction in Photosystem II, $S_{n+1} Q_a^- \rightarrow S_n Q_a$. In the same thylakoids, the concentration of Photosystem II centers active in oxygen evolution is 100 nM (1/540 Chl) and the concentration of those active in charge separation is 120 nM (1/450 Chl). Therefore, there are approximately two atrazine-binding sites per Photosystem II reaction center; one with high affinity and one with low affinity. High-affinity labelling with [^{14}C]azidoatrazine is associated with a 34.5 kDa protein, which is identified as D1, using polyclonal antisera. Low-affinity labelling with [^{14}C]azidoatrazine is associated with a 30–32 kDa protein, which is identified as D2 with the monoclonal antibody FQC3. Our findings indicate that both high- and low affinity sites are specific for Photosystem II function.

Introduction

Photosystem-specific herbicides hold many unique advantages for studies of light-driven electron transport. Their selective inhibition enables analysis of partial photosynthetic reactions, and herbicide binding is a well established tool in the quantitation of Photosystem II reaction centers. Photoaffinity labelling techniques allow identification of physiologically important proteins associated with herbicide binding. Clearly, all of these applications require rigorous understanding of the physical and mechanistic characteristics of each herbicide.

Izawa and Good [1] studied the binding of DCMU and atrazine in whole chloroplasts and correlated binding to the inhibition of Hill reaction. Two binding affinities were found, only one of which corresponded

---

The mention of firm names or trade products does not imply that they are endorsed or recommended by the U.S. Department of Agriculture over other firms or similar products not mentioned.

Abbreviations: DCMU, 3-(3,4-dichlorophenyl)-1,1-dimethylurea; atrazine, 2-chloro-4-(ethylamino)-6-(isopropylamino)-s-triazine; dinoseb, (2-(1-methylpropyl)-4,6-dinitrophenol; terbutryn: 2-(tert-butylamino)-4-(ethylamino)-6-(methylthio)-*S*-triazine; PUDF, polyvinyldifluoride; SDS, sodium dodecyl sulfate; Q_a, primary quinone acceptor in photosystem II; Q_b, secondary quinone acceptor in photosystem II; S_n, charge states of the oxygen-evolving system; Chl, chlorophyll; K_d, dissociation constant; TES, *N*-tris(Hydroxymethyl)methyl-2-aminoethanesulfonic acid; PAGE, polyacrylamide gel electrophoresis; PPO, 2,5-diphenyloxazole; kDa, kilo Dalton; SDS, sodium dodecyl sulfate; PVDF, polyvinyldifluoride; BSA, bovine serum albumin.

Correspondence: P.A. Jursinic, Plant Biochemistry Research, Northern Regional Research Center, Agricultural Research Service, U.S. Department of Agriculture, 1815 N. University St., Peoria, IL 61604, U.S.A.

to inhibition of electron flow. Tischer and Strotman [2] investigated the binding of a large number of herbicides to thylakoids (broken chloroplasts). They found that many exhibited both high- and low-affinity binding instead of a simple single-affinity binding. They called high-affinity binding 'specific' because it correlated with inhibition of electron flow; low-affinity binding was designated 'unspecific' or, as others have designated it, 'nonspecific'. The identification of multiple binding affinities for many different herbicides has been reported consistently [3–6].

The association of particular proteins with herbicide inhibition sites became possible with the synthesis of photoaffinity analogs, azidoherbicides, that combined specific physiological action with chemical reactivity sufficient to bind the herbicide covalently. Azidoatrazine [7] and azidomonuron [8] were bound primarily to a 32 kDa protein. Azido-i-dinoseb was bound to proteins in the 41 to 53 kDa range [9,10]. This association of herbicide binding with a particular protein was strengthened by study of plants that were resistant to herbicides. The primary amino acid sequence of the 32 kDa protein was determined [11]. Eventually, specific amino acid replacements were found to produce herbicide resistance [12–16]. The 32 kDa protein is considered to be one of the Photosystem II reaction center core proteins [17]. As such, quantitation of Photosystem II becomes possible via herbicide binding studies.

In spite of very exciting developments that support the concept of unique proteins with single binding sites for herbicides, a number of inconsistencies have emerged. Gressel [18] pointed out that the chemical structure of azidoatrazine could allow covalent binding to proteins other than those to which the herbicide binds noncovalently. Affinity labelling with [^{14}C]azidoatrazine and [^{14}C]azidoplastoquinone suggested that both agents bound to non-identical 32 kDa proteins [19].

Proteins other than the 32 kDa reaction center protein can bind herbicides such as the 41 kDa protein for DCMU and i-dinoseb. Enzymatic digestion of many photosystem II proteins will affect herbicide binding [6,20]. Many herbicides are known to have multiple sites of action, inhibiting reactions on the oxididizing as well as reducing side of Photosystem II [21–24]. In our study, we will correlate high and low affinity binding with specific proteins and infer their physiological function.

Correlations of herbicide binding and inhibition of electron transport have not always taken into account that the characteristics of herbicide binding change with illumination [25]. Suspect correlations include those in which the binding studies were carried out in the dark or low light while the inhibition of electron transport was determined under bright illumination. In this work, methods were developed that allowed atrazine binding and the associated inhibition of photosynthetic reactions to be studied in dark-adapted samples. High-affinity binding ('specific binding') of atrazine was correlated with blockage of the $Q_a^- Q_b \rightarrow Q_a Q_b^-$ electron transfer reaction; this corresponded with binding to a 34.5 kDa protein, and this protein was identified as the D1 protein. Low-affinity binding ('unspecific binding') of atrazine was correlated with partial inhibition of the Q_a^- recombination with oxygen evolution S-states; this corresponded with binding to a 30 kDa protein, and this protein was identified with the D2 protein. The concentration of both binding sites was found to be approximately twice that of the Photosystem II reaction center determined by oxygen evolution per flash or the absorption change of the quinone acceptor. Thus, there are two atrazine-binding sites per Photosystem II reaction center; one of high affinity and one of low affinity.

Materials and Methods

Plant material

Dwarf pea seedlings (*Pisum sativum* L. var. Progress 9) were grown in a growth chamber for approx. 4 weeks (16 h day; 25° C/20° C; light intensity, 70 W/m^2).

Thylakoid preparation

Thylakoids were prepared as previously described [26] except for a change in the order of centrifugation. Instead of a slow-speed centrifugation, a 5 min 5000 × *g* centrifugation is done immediately after homogenization and straining. This rapidly removes the thylakoids from the grinding medium. This change in procedure was found to give thylakoids with more reproducible photosynthetic characteristics. The thylakoids were suspended in a reaction media consisting of: 400 mM sucrose, 50 mM Tes (pH 7.5), 10 mM NaCl, 5 mM $MgCl_2$. Within 1 h after preparation, the thylakoids were frozen and stored in liquid nitrogen. As required, thylakoids were rapidly thawed and used immediately.

Herbicide binding

Herbicide binding was performed on dark-adapted samples as previously described [27], using [^{14}C]atrazine (Sigma, St. Louis, MO; 25 mCi/mmol). Since illumination conditions were found to alter herbicide-binding characteristics [25], all binding equilibrations were done in the dark for 10 min or longer. In our samples and experimental conditions, this is sufficient time in the dark for less than 4.4% Q_b to remain reduced [28]. The herbicide binding affinity is significantly decreased when ethanol concentrations exceed 1% (v/v) [29]. All of our herbicide additions were made such that the ethanol concentration was $\leq 1\%$ (v/v). The amount of bound inhibitor was calculated from the difference in added inhibitor with respect to

free inhibitor in the supernatant, following centrifugation of the sample. The resulting data were analyzed as described in the Appendix. It should be noted that true K_d values are obtained only in the absence of any competition. However, in thylakoids, Q_b, the secondary quinone acceptor, is present and competes with the herbicide for the binding site on D1. This caution is not exclusive to the present work but holds for most photosynthetic literature.

Fast herbicide mixing

In some experiments the sample and herbicide had to be mixed rapidly and then followed by the measurement of chlorophyll (Chl) *a* fluorescence. A mixing apparatus was constructed that consisted of two 1 ml syringes feeding into a common junction tube ('Y' tube), which passed the mixed sample into the measuring cuvette. One syringe contained 1 ml of sample at 20 μg Chl/ml and the second syringe contained 1 ml of atrazine at 20 μM, to give a final concentration of 10 μg Chl/ml and 10 μM atrazine. The syringes were hand operated, and the fastest mixing time was about 0.5 s.

Fluorescence

The Chl *a* fluorescence yield was measured by the two-flash method [30]. The actinic flash was provided by a General Radio Strobotac 1538-A through a Corning CS 4-96 glass filter. The delayed analytic flash was identical to the actinic flash, except that it was reduced in intensity 99.5% by a 0.5% transmittant neutral density filter. Chl *a* fluorescence was detected by a Hamamatsu R928 photomultiplier that was shielded from the actinic light with a Corning CS 2-64 glass filter. The photomultiplier was positioned at a right angle with respect to the direction of the flash lamps. The analog output of the photomultiplier was digitized by a Biomation model 2805 waveform recorder. Digitized data were transferred to a Hewlett Packard HP87 minicomputer, which had been programmed to determine peak heights. For the measurement of Chl *a* fluorescence light curves, the excitation flash lamp was replaced with a tungsten lamp operated with a DC power supply. The excitation intensity was altered with neutral density filters and the level of fluorescence was allowed to come to equilibrium. The analog output of the photomultiplier was monitored with a digital voltmeter.

Photoaffinity labelling

A special protocol was used in which the ultraviolet illumination step was carried out on samples at a temperature $\leq 0\,^\circ$C. Ultraviolet illumination energizes photosynthetic reactions, and this will alter the herbicide binding characteristics [25]. We found that this light-induced change in herbicide binding was greatly slowed at temperatures $\leq 0\,^\circ$C while the photoaffinity reaction continued normally. Thylakoids were suspended in reaction media at 50 μg Chl/ml. The samples were dark adapted for 5 min. [^{14}C]Azidoatrazine (Pathfinders Laboratories, St. Louis, MO; 10.26 mCi/mmol) was added and allowed to equilibrate at room temperature in the dark for 5 min. The samples were transferred to small reaction vessels, which were either imbedded in blocks of ice or packed in dry ice, and thermally equilibrated for 15 min in the dark. Samples were then illuminated for 10 min under a Spectroline shortwavelength ultraviolet lamp, 254 nm ($12 \cdot 10^3$ erg cm^{-2} s^{-1}). Following the ultraviolet illumination, the thylakoids were pelleted, solubilized and electrophoresed.

Electrophoresis

Membrane proteins were separated by gel electrophoresis in a modified Delepelaire and Chua [31] system [32]. 25 μg of Chl was loaded per lane for electrophoresis. Polyacrylamide gradients of 12 to 15% were used, molecular weight markers were included (Bio-Rad) on each gel. For urea gels, 6 M urea was included in 10% sodium dodecyl sulfate (SDS) gels or in 13 to 15% SDS step gels. Following electrophoresis, Coomassie-stained gels were either treated with PPO/DMSO and dried onto Whatman 3MM filter paper where positions of the molecular weight markers were indicated with radioactive ink and fluorographed [33,34] at $-80\,^\circ$C for 1 to 12 weeks or the appropriate bands were sliced from the gels, digested with NCS (Amersham) and counted by liquid scintillation. When the gel was to be digested, the protein bands from two lanes or 50 μg Chl were collected for each [^{14}C]azidoatrazine concentration.

Antibody detection

The identity of the D1 and D2 components were verified immunologically. After electrophoresis, the proteins were electrophoretically transferred [35] to a PVDF membrane (Immobilon, Millipore). The membrane was then blocked with 5% non-fat dry milk dissolved in 10 mM Tris-HCl (pH 7.4) containing 150 mm NaCl (TS buffer) for 4 h at room temperature. After extensive washing with TS buffer, sections of the immunoblot were incubated with either an anti-D1 polyclonal antisera (diluted 1:4000 in TS buffer containing 1% bovine serum albumin (BSA)) or an anti-D2 monoclonal antibody, FQC3 (diluted 1:2000 in TS buffer containing 1% BSA). After incubation overnight at room temperature, the immunoblots were washed extensively with TS buffer and incubated with either an anti-rabbit IgG-peroxidase conjugate (for the anti-D1 primary antibody) or an anti-mouse IgG-peroxidase conjugate (for FQC3). Both of these secondary antibodies were diluted 1:1000 in TS buffer containing 1%

BSA and incubated for 4 h at room temperature. After incubation, the blots were washed extensively with TS buffer and developed with 4-chloro-1-naphthol + H_2O_2 [36].

Results

The characteristics of atrazine binding as a function of concentration are presented in Fig. 1. The double reciprocal plot has a biphasic shape and is similar to results reported by Tischer and Strotman [2]. This type of plot will be linear if there is a single binding site and curved or biphasic if there are multiple binding sites with different dissociation constants [37]. To convince ourselves of the nonlinearity of this data, many points were taken at high concentration of atrazine and are plotted in Fig. 2. A linear extrapolation of the high affinity portion of Fig. 1 (12 to 40 nM free atrazine), which is a presumption of a single binding site of high affinity, is shown as a broken line and clearly is an inadequate model for this data.

An analysis of the data in Fig. 1 was carried out as described in the Appendix. From the ordinate intercept, I_2, the concentration of the total number of binding sites was calculated to be 240 ± 24 nM (1 site/240 Chl). The indicated uncertainty is the standard deviation for five repeat measurements. The best fit to the data occurred with two binding sites of equal concentration $n_1 = n_2 = 120 \pm 24$ nM. One site had high affinity with a $K_d = 80 \pm 9$ nM and the other site had low affinity with a $K_d = 420 \pm 100$ nM. Fig. 3 shows the amount of atrazine bound to each of these sites as a function of added atrazine concentration. At the highest atrazine concentration in Fig. 2, which is 1.1 μm free atrazine, the high affinity site is 94% saturated and the low affinity site was 77% saturated.

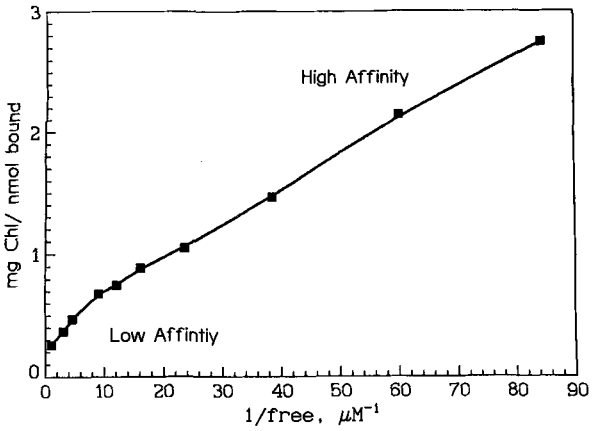

Fig. 1. Binding of [^{14}C]atrazine to dark-adapted thylakoids at a concentration of 50 μg Chl/ml. A plot of 1/bound to 1/free atrazine is shown that allows the calculation of the number of binding sites and the dissociation constants, see the Appendix for details of this mathematical analysis.

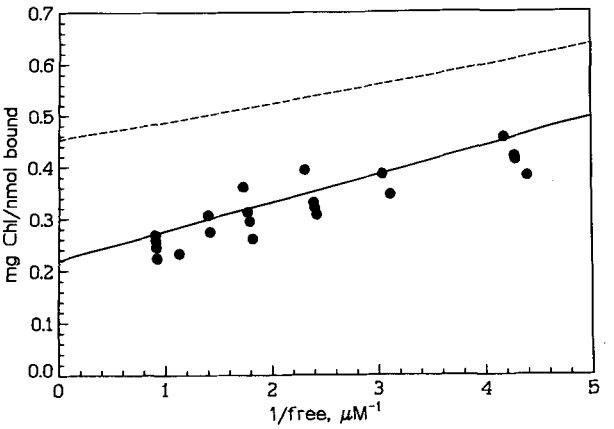

Fig. 2. Binding of [^{14}C]atrazine to dark-adapted thylakoids at a concentration of 50 μg Chl/ml. A plot of 1/bound to 1/free atrazine is shown for free atrazine concentrations above 200 nM. Data are shown as plotted points. The broken line is a linear extrapolation of the high affinity portion (12 to 40 nM free atrazine) portion of Fig. 1. The solid line is the predicted data based on a model having a high affinity site of concentration 120 nM and dissociation constant of 80 nM and a low affinity site of concentration 120 nM and dissociation constant of 420 nM.

These curves were calculated by using Eqn. 1 of the Appendix and the parameters for the high and low affinity sites. When flash excitation methods [38] were used with the same sample, the concentration of Photosystem II centers active in oxygen evolution was 100 ± 6 nM (1/540 Chl) and the concentration of centers active in charge separation was 120 ± 7 nM (1/450 Chl). From these data, we conclude that there is one high-affinity and one low-affinity binding site for atrazine per Photosystem II reaction center.

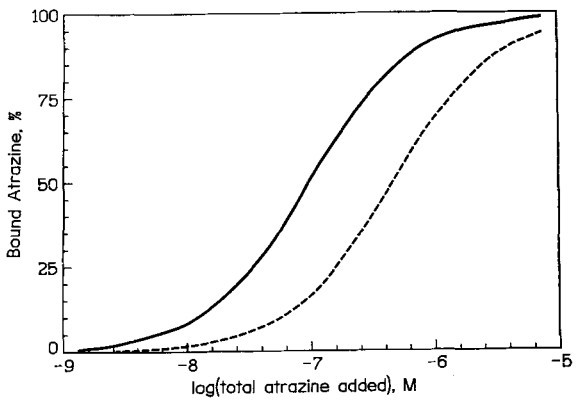

Fig. 3. The percent of atrazine bound to each of two independent sites versus the concentration of atrazine added. These plots were calculated for sample concentration of 10 μg Chl/ml (11.1 nM), using equation 1 in the Appendix and parameters derived from the data in Fig. 1. The high-affinity site (———) had a dissociation constant of 80 nM and a concentration of 23.8 nM, and the low-affinity site (— — —) had a dissociation constant of 420 nM and a concentration of 23.8 nM. The concentration of added atrazine for 50% binding was 95 and 450 nM for the high- and low-affinity sites, respectively.

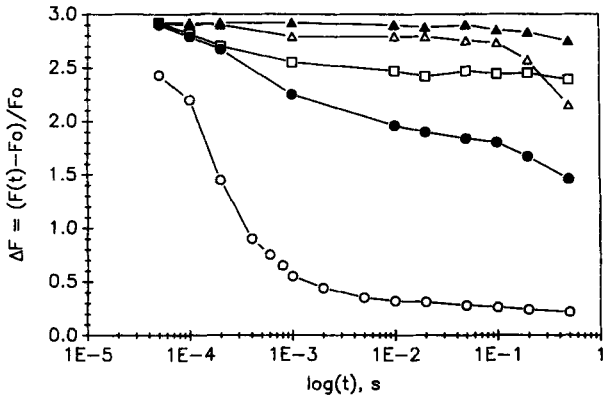

Fig. 4. The decay of variable Chl *a* fluorescence versus time after a single flash. $F(t)$ is the fluorescence amplitude at time t after a flash, and F_0 is the fluorescence amplitude of a dark-adapted sample. Decays are shown for control (○——○); plus 350 nM atrazine with (□——□) or without (●——●) 5 μM hydroxylamine; plus 10 μM atrazine with (▲——▲) or without (△——△) 5 mM hydroxylamine. The sample concentration was 10 μg Chl/ml, and the sample was dark-adapted for 10 min or longer. When atrazine was added 2 min incubation time was allowed before measurements were made.

In earlier work Tischer and Strotman [2] also found that atrazine had two binding affinities denoted as specific and unspecific binding. Their nomenclature recognized two types of inhibitor interactions, but related inhibition of electron flow only to the high-affinity or specific-binding site. The low-affinity site was assumed to be unspecific binding, having no discernible Photosystem II function. Our experience indicates that binding data and atrazine inhibition of Photosystem II reactions must be compared carefully in order to discover the function for the low-affinity binding. A major difficulty in making such comparisons is that photosynthetic reactions are measured in light, and illumination alters herbicide-binding characteristics [25]. This problem can be circumvented by using the decay of the Photosystem II-dependent variable component of Chl *a* fluorescence as a measure of photosynthetic activity. With this fluorescence technique, herbicide binding comes to equilibrium in a dark-adapted sample just as in the [^{14}C]atrazine-binding studies, and the effects of binding of Photosystem II charge separation and electron flow are assessed by monitoring Chl *a* fluorescence, which is measured after a single saturating excitation flash.

The level of variable Chl *a* fluorescence corresponds to the extent of Q_a reduction [39]. Fig. 4 shows the decay of Chl *a* fluorescence, Q_a^- oxidation, with time after a single flash under different experimental conditions. Decay in the microsecond and millisecond range corresponds to Q_a^- reoxidation by electron transport to Q_b, $Q_a^-Q_b \rightarrow Q_aQ_b^-$ [40,41]. In the control, this reaction occurs in all centers and most of the decay takes place in less than 5 ms. With 350 nM atrazine present, the decay is much slower with only a small portion occurring at less than 5 ms, which corresponds to unfilled binding sites, see Fig. 3. With 10 μM atrazine present, 98% of the sites have atrazine bound and as expected very little decay occurs at times less than 5 ms.

Decay of Chl *a* fluorescence in the seconds range corresponds to Q_a^- reoxidation by charge recombination with oxygen evolution S-states, $S_2Q_a^- \rightarrow S_1Q_a$ [42–45]. The major component of this recombination reaction has a 1 to 2 s half-time [44,45]. In Fig. 4, the samples with 350 nM and 10 μM atrazine present have decay components in the hundreds of milliseconds and seconds range, which we believe are due to charge recombination. This is shown in Fig. 4 by comparing decay in the sample with 350 nM atrazine present with (□——□) and without (●——●) hydroxylamine and in samples with 10 μM atrazine present with (▲——▲) and without (△——△) hydroxylamine. The generation of S-states is blocked by the presence of hydroxylamine [46], which eliminates the $S_2Q_a^- \rightarrow S_1Q_a$ recombination reaction. The presence of hydroxylamine slows the decay of Q_a^- in the hundreds of milliseconds and seconds range. The amount of recombination, the difference between the decay with and without hydroxylamine, is less in the sample with 10 μM atrazine present than in the sample with 350 nM atrazine present. This is interpreted to mean that with 10 μM atrazine present, when the low affinity site is filled with atrazine, the recombination reaction is partially blocked. In other words, it appears that the higher concentration of atrazine acts like hydroxylamine treatment in slowing the fluorescence decay in the tens and hundreds of milliseconds range. We interpret this to mean that the higher concentrations of atrazine partially blocks the $S_2\ Q_a^- \rightarrow S_1Q_a$ charge recombination reaction.

The decay that occurs between 1 and 10 s in the hydroxylamine plus 10 μM atrazine sample is likely due to exchange of atrazine from the binding site giving the following reaction: $Q_aI + Q_b \rightarrow Q_a^- + I + Q_b \rightarrow Q_a^-Q_b + I \rightarrow Q_aQ_b^- + I$. The half-time of this exchange of atrazine is estimated to be 32 s from the Chl *a* fluorescence decay in Fig. 4.

The effect of atrazine on electron transport was monitored by measuring Chl *a* fluorescence 100 ms after a single actinic flash given to dark-adapted thylakoids as a function of atrazine concentration (Fig. 5). The data can be described by a single binding site with a dissociation constant of 80 nM (——), which misses points at low concentrations as expected from the non-linear relationships between Q_a^- and variable fluorescence in thylakoids. A single binding site with a dissociation constant of 420 nM (— — —) is a poor fit of the data. From the data we conclude that only the

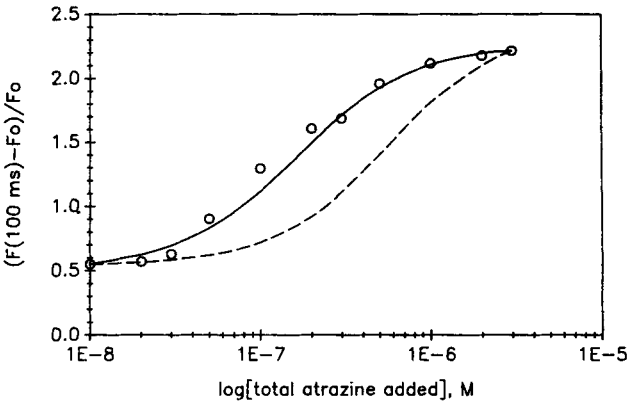

Fig. 5. The variable Chl *a* fluorescence, $\Delta F(100\text{ ms}) = (F(100\text{ ms}) - F_0)/F_0$, measured 100 ms after a flash versus the concentration of added atrazine. Atrazine was added to a dark-adapted sample and allowed to equilibrate for 10 min in the dark prior to the measurement of fluorescence. F_0 is the Chl *a* fluorescence measured in the dark-adapted sample prior to any flash excitation. The Chl *a* fluorescence, $F(100\text{ ms})$, is measured 100 ms after a single saturating-xenon flash. The sample concentration was 10 μg Chl/ml. The data points are shown as ○. Calculated curves are shown for the variable fluorescence being a function of herbicide binding to various sites. The solid curve (———) is for a site with a dissociation constant of 80 nM and concentration of 1 site/480 Chl. The dashed curve (— — —) is for a site with a dissociation constant of 420 nM and a concentration of 1 site/480 Chl.

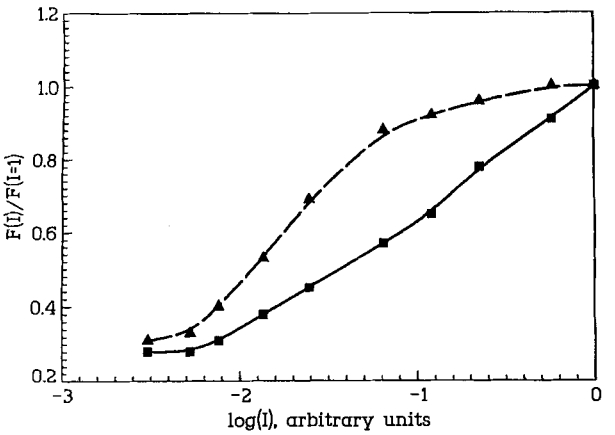

Fig. 6. The level of Chl *a* fluorescence versus the intensity of applied continuous light. $F(I)$ is the fluorescence level at light intensity I and $F(I=1)$ is the fluorescence level at full-light intensity. Light curves are for a sample with 350 nM atrazine (■ ——— ■), and 10 μM atrazine (▲ ——— ▲) present. The sample was at a concentration of 10 μg Chl/ml.

high-affinity site controls electron flow between $Q_a^- Q_b \rightarrow Q_a Q_b^-$.

This idea of atrazine inhibition of electron flow and charge recombination was further tested by measuring variable fluorescence versus the intensity of applied continuous light in the presence of 350 nM atrazine, which blocks 75% of $Q_a^- Q_b \rightarrow Q_a Q_b^-$ but allows equilibrium between the forward light reaction that produces Q_a^- and high fluorescence and the backward dark reaction ($S_2 Q_a^- \rightarrow S_1 Q_a$) that produces Q_a and low fluorescence. Light curves are shown in Fig. 6, for 350 nM and 10 μM atrazine. In 10 μM atrazine, the light curve is shifted to lower intensities, which is consistent with complete blockage of $Q_a^- Q_b \rightarrow Q_a Q_b^-$ and inhibition of the $S_2 Q_a^- \rightarrow S_1 Q_a$ recombination.

The two binding sites have been distinguished by their binding affinities in Figs. 1 and 2. Another possible difference between these sites might be the rate at which atrazine binds to them. Accordingly, 10 μM atrazine was added with rapid mixing, and Chl *a* fluorescence was measured 100 ms after a flash given at various times after the addition. Binding to the high-affinity site, which blocks $Q_a^- Q_b \rightarrow Q_a Q_b^-$ and slows fluorescence decay (Fig. 4), was detected as a rise in Chl *a* fluorescence. This technique was first used by Lavergne [47] to determine the rate of DCMU binding. Here, high-affinity binding was distinguished from binding to the low-affinity site, which inhibits recombination, by using hydroxylamine-treated samples that have millisecond and longer recombination blocked [42,47]. The rapid rise in $\Delta F(100\text{ ms})$ in Fig. 7 indicates that atrazine is almost totally bound to the high-affinity site within 1 s and thus binds to half of the sites in less than 0.5 s. This is in good agreement with the 150 ms half-time found for DCMU [47]. When a control (not hydroxylamine-treated) sample is used, the $\Delta F(100\text{ ms})$ rises slowly to a maximum at about 1 min after atrazine addition. Since recombination can take place in the control sample, the data can be explained as follows. At 1 s after 10 μM atrazine addition, the high-affinity site has atrazine bound and the $Q_a^- Q_b \rightarrow Q_a Q_b^-$ reaction is blocked, but the low-affinity site remains unbound, and the recombination reaction, $S_{n+1}\ Q_a^- \rightarrow$

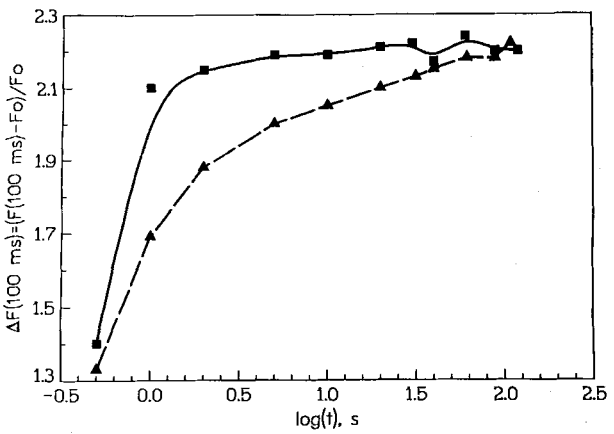

Fig. 7. The variable Chl *a* fluorescence, $\Delta F(100\text{ ms}) = (F(100\text{ ms}) - F_0)/F_0$, measured 100 ms after a flash, versus the logarithm of time, t, after addition of 10 μM atrazine. Data are for a control sample (▲ - - - ▲) and a sample treated with 5 mM hydroxylamine in the dark for 1 min (■ ——— ■). All other symbols and conditions are defined in the legend of Fig. 5.

S_nQ_a, occurs. Therefore, at 1 s after addition, ΔF(100 ms) = 1.7 and is not maximal because the recombination reaction partially oxidizes Q_a^-. At longer times after atrazine addition, ΔF(100 ms) increases, reaching a maximum of 2.2 at 1 min or longer. This rise in ΔF(100 ms) from 1.7 to 2.2 between 1 and 30 s after atrazine addition corresponds to an inhibition of the recombination reaction as the low-affinity site becomes bound with atrazine. The data of Fig. 7 show that the low-affinity site is filled with a half-time of 4 to 5 s.

In 1981 Gardner [48] developed techniques for covalent linkage of atrazine to thylakoid membrane proteins using [^{14}C]azidoatrazine under ultraviolet illumination. Such photoaffinity labels can appear to link nonspecifically when the label concentration is high, but correlations of labelling with physiological function are reasonable when care has been exercised in the labelling protocol. Mullet and Arntzen [49] correlated herbicide binding to a 34 kDa protein with a block in the $Q_a^-Q_b \rightarrow Q_aQ_b^-$ reaction. It is clear from Figs. 1 to 5 that another atrazine-binding site exists in photosystem II. There are at least two possible ways to explain multiple sites for the physical binding of atrazine with thylakoid proteins. There may be more than one binding site on a single protein, or there may be more than one protein with an atrazine-binding site. To test these possibilities, we started with standard photoaffinity tagging by [^{14}C]azidoatrazine [48,7,50]. Fluorography of separated thylakoid proteins (Fig. 8) indicated two prominent bands, one at 34.5 kDa; the second at 30 kDa. There were also a few very light bands at 23 kDa. The 34.5 kDa protein was most heavily labelled. Based on the apparent molecular masses in SDS gels of these two photoaffinity labelled proteins, the 34.5 kDa protein appears to be D1 and the 30 kDa protein appears to be D2 [20,49].

This was confirmed by the different migration of these two proteins in urea and non-urea containing SDS-PAGE. It has been shown [20] that in SDS gels without urea the D2 protein exhibits higher mobility than the D1 protein. In SDS gels with urea, these mobilities are reversed with the D1 protein migrating faster than the D2 protein. Fig. 9A shows a fluorograph of azidoatrazine-labelled proteins separated on a 10% SDS urea gel. It is clear that the heavily atrazine-labelled band runs with a higher mobility in this urea gel than the lightly-labelled band. This is the reverse of what is found in the SDS gels without urea, Fig. 8, and is evidence for identifying the heavily atrazine-labelled band with the D1 polypeptide and the lightly-labelled band with the D2 polypeptide.

Additional confirmation of this identification comes from immunoblot analysis. Thylakoid proteins were separated on a 12 to 15% step polyacrylamide gradient gel containing 6 M urea. The proteins were electrophoretically transferred to a PVDF membrane and

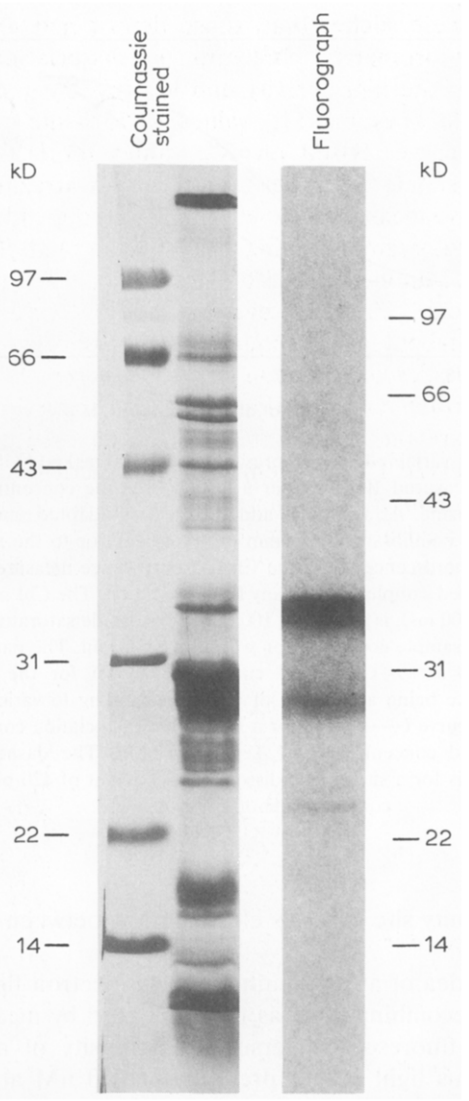

Fig. 8. Photoaffinity labelling of pea thylakoids membranes with 1.19 μM [^{14}C]azidoatrazine. Dark-adapted and -equilibrated samples were thermally equilibrated at $\leq 0°$ before ultraviolet irradiation. The labelled proteins were separated by electrophoresis with a 12–15% SDS gradient-polyacrylamide gel. Left, a Coomassie stained gel; right, a four week fluorograph of a similar gel. Molecular weight standards: rabbit phosphorylase B, bovine serum albumin, hen ovalbumin, bovine carbonic anhydrase, soybean trypsin inhibitor, and hen lysozyme.

reacted with anti-D1 polyclonal antibody and a D2-specific monoclonal antibody, FQC3 [51]. Fig. 9B and C shows the D1 and D2 antibody labelling after separation in urea-containing gels. The band with highest mobility is labelled by the D1 antibody, and the band with lower mobility is labelled by the D2 antibody. There also is a band high on the gel that has very low mobility and is labelled by both the D1 and D2 antibody. This band is a putative D1/D2 heterodimer [51].

A standard binding curve generated with [^{14}C]azidoatrazine was biphasic like that for atrazine (Fig. 1), but dissociation constants for azidoatrazine (data not

shown) were higher than those determined for atrazine. Unfortunately azidoatrazine dissociation constants for the high affinity and low affinity sites were too similar to estimate I_{50} values for each site from the binding curve. Based on K_d values for [^{14}C]azidoatrazine should be higher than those for atrazine.

We also measured the concentration-dependence of [^{14}C]azidoatrazine binding to the 34.5 and 30 kDa proteins. Illumination shifts the binding characteristics of herbicides [25], so care was taken to develop a covalent-labelling technique that would preserve the characteristics of dark-equilibrated samples. This was an important consideration since it was our intention to compare binding affinities of the labelled proteins with observed Photosystem II-specific activities. By irradiating samples that were frozen with solid CO_2 in a dark-adapted and pre-equilibrated state, we were able to achieve nearly identical equilibrium results for ultraviolet irradiated samples. Pea thylakoids were covalently labelled in this manner, proteins were then separated by gel electrophoresis, sliced from the gel, digested and counted. Fig. 10 presents the results. The scatter in the data of this figure does not allow strong conclusions to be made. However, at 3 μM azidoatrazine, the 34.5 kDa protein is 95% saturated while at 13 μM the 30 kDa protein is still binding additional azidoatrazine. The 34.5 kDa protein was the first site to saturate with [^{14}C]azidoatrazine. The apparent I_{50} was 200 nM. Binding at this site blocked the $Q_a^- Q_b \rightarrow Q_a Q_b^-$ reaction. Thus, the 34.5 kDa appears to be the D1 protein of Mullet and Arnzten [49]. Binding at the low-affinity site indicates that the 30 kDa protein has an apparent I_{50} of 800 nM. Inhibition of the charge recombination, $S_{n+1}Q_a^- \rightarrow S_nQ_a$, is the Photosystem II function for this site.

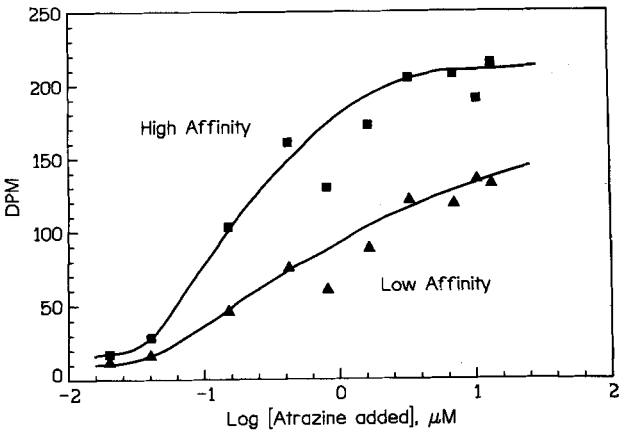

Fig. 10. [^{14}C]Azidoatrazine concentration-dependent labelling of the 34.5 (■ ——— ■) and 30 kDa (▲ ——— ▲) proteins. The concentration of [^{14}C]azidoatrazine was varied from 0.02 to 13.4 μM. Following covalent linkage the proteins were separated by SDS gel electrophoresis. Appropriate bands were sliced out of the gels, digested with NCS, and counted by liquid scintillation.

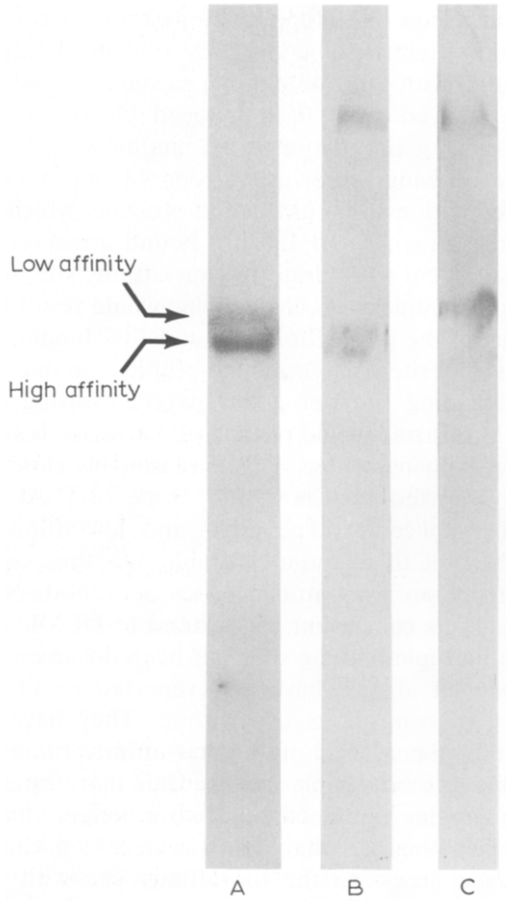

Fig. 9. Photoaffinity and monoclonal antibody labelled SDS urea gels. (A) Thylakoid proteins that were photoaffinity labelled with [^{14}C]azidoatrazine were run on a 10% SDS, 6 M urea gel. A fluorograph of this gel is shown. (B) D1 monoclonal antibody labelling of a poly(vinyldifluoride) membrane that had thylakoid proteins electrophoretically transferred to it from a 13 to 15% step SDS, 6 M urea gel. (C) Same as B except D2 monoclonal antibody labelling was done.

Discussion

Atrazine binds to whole algal cells [1] and thylakoids [2,6] with high- and low-affinity. While much attention has been devoted to high-affinity binding and the nature of the high-affinity binding site [2,7,11,52,49,12], low-affinity binding has been considered 'unspecific' [2] and accorded much less attention. Speculation regarding the nature of low-affinity binding has suggested partitioning into lipophilic membranes [6], binding to LHCP proteins [49], and binding to the sides of tubes [10]. We have found, however, that the low-affinity site has a specific K_d of binding, is associated with a 30–32 kDa protein, and when bound with atrazine, charge recombination with the oxygen-evolving S-states, $S_{n+1}Q_a^- Q_b \rightarrow S_nQ_aQ_b$ is partially blocked. Atrazine, bound at the low-affinity site, also blocks bicarbonate

binding at one of its sites on photosystem II [53]. Therefore, we suggest that low-affinity binding is photosystem II specific.

The sites of high- and low-affinity binding have been identified as being distinct. The high affinity site has a $K_d = 80$ nM, is present at a concentration of 1 site/470 Chl, binds in less than 500 ms, blocks the electron flow reaction $Q_a^- Q_b \rightarrow Q_a Q_b^-$, and binds to the D1 photosystem II protein. The low affinity site has a $K_d = 420$ nM, is present at a concentration of 1 site/470 Chl, binds with a half time of 4 to 5 s, partially inhibits the charge recombination reaction in photosystem II ($S_{n+1} Q_a^- \rightarrow S_n Q_a$), and binds to the D2 Photosystem II protein. The identification of the high and low affinity binding sites with the D1 and D2 Photosystem II proteins is based on three pieces of evidence. The migration on SDS gels of proteins with covalently bound atrazine correspond to the molecular mass of the D1 and D2 proteins for the high-affinity and low-affinity binding sites. When these proteins are run on SDS-urea gels, their migration position reverses, which is characteristic of the D1 and D2 proteins. The labelling of these proteins with monoclonal antibodies is specific to D1 and D2.

One possible difficulty in the assignment of azidoatrazine labelling of proteins could arise from the rapid turnover of the D1 protein [54,55], which might produce large pools of D1 precursor. It could be argued that the observed low-affinity binding we observe results from attachment of [^{14}C]azidoatrazine to precursor-D1 molecules. This difficulty can be dismissed based on recent work by Wettern [56], who found two types of D1. A precursor type located in unstacked thylakoid membranes, the stroma lamella, amounted to 30–35% of the total D1 protein, but did not bind azidoatrazine [56]. Only fully incorporated D1 in the stacked grana membranes binds azidoatrazine.

Another possible problem is that the 30 kDa labelled protein might be a degraded D1 protein product in the membrane and not a second atrazine receptor. Azidoatrazine does not bind to membrane-bound precursor D1 [56], and there is no evidence that azidoatrazine will bind to degraded D1 fragments. The possibility remains that azidoatrazine binds to intact D1 that is subsequently degraded on handling or by in vivo mechanisms. This latter explanation for the 30 kDa protein seems unlikely for the following reason. The reported primary in vivo and in vitro degradation product of D1 is a 23.5 kDa protein [57,58]. We see very slight labelling in this molecular weight range (Fig. 8).

The binding of DCMU to a site that blocks $Q_a^- Q_b \rightarrow Q_a Q_b^-$ occurs with a 150 ms half-time [47]. We find that 10 μM atrazine binds to a high-affinity site and blocks $Q_a^- Q_b \rightarrow Q_a Q_b^-$ with a half-time of less than 500 ms, Fig. 7. In addition, we find that 10 μM atrazine binds to a low-affinity site, which partially blocks the recombination reaction $S_{n+1} Q_a^- \rightarrow S_n Q_a$, with a half-time of 4 to 5 s, Fig. 7. The two binding sites can be distinguished by binding time as well as binding affinity.

This dual effect of atrazine is very similar to the effect of anions at anion binding site II [59]. With no anions added or bicarbonate added, the $Q_a^- Q_b \rightarrow Q_a Q_b^-$ reaction is rapid [59] and delayed fluorescence (recombination) is high [60]. With the addition of many anions other than bicarbonate, the $Q_a^- Q_b \rightarrow Q_a Q_b^-$ reaction is greatly slowed [59] and delayed fluorescence (recombination) is low [60]. The binding of atrazine or anions other than bicarbonate thus change the Q_a, Q_b environment in some way that slows electron transfer as well as decreases charge recombination.

Investigations of physiological adaptation to environment have given much attention to changes in the stoichiometric ratio of photosystem I to photosystem II. One method commonly used in measuring photosystem II relies on atrazine binding. Erroneous estimates can be made if the two binding sites are not taken into account. Chow and Hope [61] found the concentration of Photosystem II to be larger by a factor of 1.21 when measured with atrazine binding as compared with estimates derived from flash induced O_2 or H^+ yield. They did not find two atrazine binding sites for every oxygen evolving center as we report here. We believe their conditions (400 nM added atrazine, which is 270 nM free atrazine and 130 nM bound atrazine) would be insufficient to saturate the low-affinity site, see Fig. 3. In our samples, 400 nM atrazine would result in 82% binding to the high-affinity site and 47% binding to the low-affinity site. With one high-affinity and one low-affinity binding site per active oxygen-evolving center, 400 nM atrazine would result in 1.3 atrazine bound per oxygen-evolving center. This is reasonably close to the value reported by Chow and Hope [61]. At higher atrazine concentrations, high- and low-affinity sites both become filled and measurable. We, thus, conclude that there are two atrazine sites per Photosystem II center. This conclusion may extend to DCMU [3], for which multiple-binding sites has been documented.

Chow et al. [29] have now reported results, using higher concentrations of atrazine. They have found that the appearance of the low-affinity binding was variable in their samples and became more extensive if their samples remained on ice for longer than 1 h. They hypothesized that this was due to a change in herbicide access to the low-affinity site with sample treatment. In earlier work [28] the low-affinity binding site for atrazine was not always apparent. However, in our present samples that are on ice for less than 1 h, we consistently find low-affinity atrazine binding. Differences in our methods of thylakoid preparation must cause this difference in atrazine accessibility to the low-affinity site. Also we have now used higher concen-

trations of atrazine, which manifests the low-affinity site.

Several studies associate the psbA gene product, D1, with atrazine resistance [11,62,16,3,12], high-affinity atrazine binding, and the inhibition of electron flow. We propose that a low-affinity atrazine site, which can regulate charge recombination, resides on the D2 counterpart of the D1 protein. Homology between D1 and D2 [17] supports this possibility. Further work is in progress to test this thesis.

Acknowledgements

The authors wish to thank Dr. Steven Theg for his helpful reading of the manuscript and Dr. A. Trebst for providing the anti-D1 antisera. Partial support for this research was provided by NSF Grant DMB 90-06552 to T.M.B.

Appendix

This is a mathematical description of binding to multiple independent binding sites based on a more thorough treatment by Klotz and Hunston [37].

For a single binding site, the following reaction equation can be written: $S + I \leftrightarrow SI$, where S is a specific-bindiing site, I is the inhibitor and SI is the site with the bound inhibitor. From this simple model the following equilibrium equation can be written:

$$K = \frac{[n - B][F]}{[B]}$$

where K is the dissociation constant, $[n]$ is the concentration of total binding sites, [F] is free inhibitor concentration and [B] is the concentration of inhibitor-bound sites. Rearranging this equation, one obtains the familiar equation:

$$[B] = \frac{n \cdot [F]}{K + [F]} \quad \text{or} \quad \frac{1}{[B]} = \frac{K}{n} \cdot \frac{1}{[F]} + \frac{1}{n}$$

for a single specific-binding site. A plot of $1/[B]$ versus $1/[F]$ gives a straight line with an ordinate intercept of $1/n$ and an abscissa intercept of $-1/K$.

If multiple-binding sites are present with different dissociation constants, then a plot of $1/[B]$ versus $1/[F]$ will give a multiple slope plot such as seen in Fig. 1. The equation for m multiple, independent binding sites is the following:

$$[B] = \sum_{i=1}^{m} \frac{n_i[F]}{K_i + [F]} \tag{1}$$

where K_i and n_i are the dissociation constant and concentration, respectively, of the i^{th}-binding site.

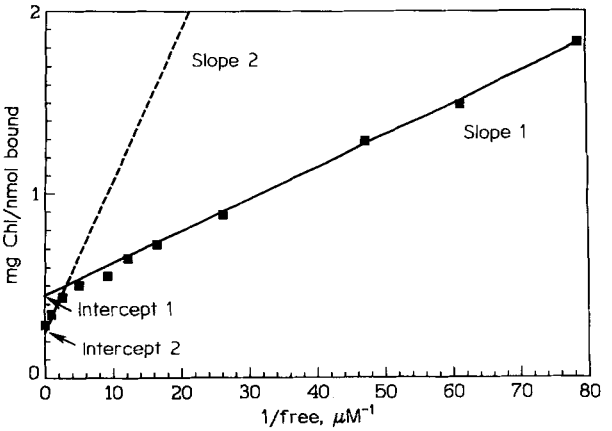

Fig. 11. Theoretical binding data for two independent-binding sites with different binding affinities. Slopes and intercepts shown for different binding curve segments are defined in the Appendix.

For a simple case of two independent-binding sites a $1/[B]$ versus $1/[F]$ plot will appear as shown in Fig. 11.

Intercept 2:

$$\text{Intercept 2} = \lim_{1/[F]\to 0}(1/[B]) = \left[\sum_{i=1}^{2} \frac{n_i[F]}{K_i + [F]}\right]^{-1}$$

$$= [n_1 + n_2]^{-1} = \frac{1}{n_1 + n_2} \tag{2}$$

Slope 1:

$$\lim_{1/[F]\to\infty} \frac{d(1/[B])}{d(1/[F])} = \frac{-1\left[\sum_{i=1}^{2} \frac{-n_i K_i[F]^2}{(K_i + [F])^2}\right]}{\left[\sum_{i=1}^{2} \frac{n_i[F]}{K_i + [F]}\right]^2}$$

$$= \frac{\left[\sum_{i=1}^{2} \frac{n_i K_i}{(K_i + [F])^2}\right]}{\left[\sum_{i=1}^{2} \frac{n_i}{K_i + [F]}\right]^2}$$

$$= \frac{\sum_{i=1}^{2} \frac{n_i}{K_i}}{\left[\sum_{i=1}^{2} \frac{n_i}{K_i}\right]^2} = \frac{1}{\sum_{i=1}^{2} \frac{n_i}{K_i}} = \frac{1}{\frac{n_1}{K_1} + \frac{n_2}{K_2}}$$

$$= \frac{K_1 K_2}{n_1 K_2 + n_2 K_1} \tag{3}$$

Slope 2:

$$\lim_{1/[F]\to 0} \frac{d(1/[B])}{d(1/[F])} = \frac{\sum_{i=1}^{2} \frac{n_i K_i}{[F]^2}}{\left[\sum_{i=1}^{2} \frac{n_i}{[F]}\right]^2} = \frac{n_1 K_1 + n_2 K_2}{(n_1 + n_2)^2} \tag{4}$$

Using the symbols I_2, S_1, S_2 for intercept 2, slope 1 and slope 2, respectively, the following relationships are useful:

From Eqns. 2 and 4 $S_2 = (n_1K_1 + n_2K_2)(I_2)^2$

$$K_2 = \frac{(S_2)}{n_2(I_2)^2} - \frac{n_1K_1}{n_2} = \frac{(n_1+n_2)^2S_2}{n_2} - \frac{n_1K_1}{n_2}$$

From Eqn. 3 $K_1K_2 = S_1(n_1K_2 + n_2K_1)$

$$K_1\left[\frac{(S_2)}{n_2(I_2)^2} - \frac{n_1K_1}{n_2}\right] = n_1S_1\left[\frac{(S_2)}{n_2(I_2)^2} - \frac{n_1K_1}{n_2}\right] + n_2S_1K_1$$

$$\frac{n_1}{n_2}K_1^2 + \left[n_2S_1 - \frac{(n_1)^2S_1}{n_2} - \frac{S_2}{n_2(I_2)^2}\right]K_1 + \frac{n_1S_1S_2}{n_2(I_2)^2} = 0$$

Various values of n_1 and n_2 are presumed and the value of K_1 is determined from the quadratic equation, and K_2 is determined by using Eqn. 3 or 4. Using these values of n_1, n_2, K_1 and K_2 and Eqn. 1, the amount of bound atrazine could be predicted for values of free atrazine. The sum of differences and sum of squared differences between the predicted and measured values for bound atrazine were calculated. The values of n_1, n_2, K_1 and K_2 that give the least sum of differences and least sum of squared differences are taken as the binding parameters.

References

1 Izawa, S. and Good, N.E. (1965) Biochim. Biophys. Acta 102, 20–38.
2 Tischer, W. and Strotman, H. (1977) Biochim. Biophys. Acta 460, 113–125.
3 Pfister, K., Radosevich, S.R. and Arntzen, C.J. (1979) Plant Physiol. 64, 995–999.
4 Trebst, A. (1979) Z. Naturforsch. 34C, 986–991.
5 Oettmeier, W. and Masson, K. (1980) Pestic. Biochem. Physiol. 14, 86–97.
6 Laasch, H., Pfister, K. and Urbach, W. (1981) Z. Naturforsch. 36C, 1041–1049.
7 Pfister, K., Steinback, K.E., Gardner, G. and Arntzen, C.J. (1981) Proc. Natl. Acad. Sci. USA 78, 981–985.
8 Boschetti, A., Tellenbach, M. and Gerber, A. (1985) Biochim. Biophys. Acta 810, 12–19.
9 Oettmeier, W., Masson, K. and Johanningmeier, U. (1980) FEBS Lett. 118, 267–270.
10 Giardi, M.T., Marden, J.B. and Barber, J. (1988) Biochim. Biophys. Acta 934, 64–71.
11 Zurawski, G., Bohnert, H.J., Whitfield, P.R. and Bottomley, W. (1982) Proc. Natl. Acad. Sci. USA 79, 7699–7703.
12 Erickson, J.M., Rahire, M., Bennoun, P., Delepelaire, P., Diner, B. and Rochaix, J.D. (1984) Proc. Natl. Acad. Sci. USA 81, 3617–3621.
13 Erickson, J.M., Rahire, M., Rochaix, J.D. and Mets, L. (1985) Science 228, 204–207.
14 Sinclair, J. and MacDonald, P. (1987) Can. J. Bot. 65, 2147–2151.
15 Hirschberg, J., Bleecker, A., Kyle, D.J., McIntosh, L. and Artnzen, C.J. (1984) Z. Naturforsch. 39C, 412–420.
16 Wolber, P.K. and Steinback, K.E. (1984) Z. Naturforsch. 39C, 425–429.
17 Hearst, J.E. and Sauer, K. (1984) Z. Naturforsch. 39C, 421–424.
18 Gressel, J. (1982) Plant Sci. Lett. 25, 99–106.
19 Oettmeier, W., Soll, H.J. and Neumann, E. (1984) Z. Naturforsch. 39C, 393–396.
20 Marder, J.B., Chapman, D.J., Telfer, A., Nixon, P.J. and Barber, J. (1987) Plant Mol. Biol. 9, 325–333.
21 Renger, G. (1973) Biochim. Biophys. Acta 314, 113–116.
22 Etienne, A.L. (1974) Biochim. Biophys. Acta 333, 320–330.
23 Van Assche, C.J. (1984) Z. Naturforsch. 39C, 338–341.
24 Vasil'ev, I.R., Matorin, D.N., Lyadsky, V.V. and Venediktov, P.S. (1988) Photosyn. Res. 15, 33–39.
25 Jursinic, P. and Stemler, A. (1983) Plant Physiol. 73, 703–708.
26 Jursinic, P. (1978) FEBS Lett. 90, 15–20.
27 Jursinic, P. and Dennenberg, R. (1985) Arch. Biochem. Biophys. 241, 540–549.
28 Jursinic, P. and Dennenberg, R. (1988) Biochim. Biophys. Acta 935, 225–235.
29 Chow, W.S., Hope, A.B. and Anderson, J.M. (1990) Phytosyn. Res. 24, 109–113.
30 Jursinic, P., Warden, J. and Govindjee (1976) Biochim. Biophys. Acta 440, 322–330.
31 Delepelaire, P. and Chua, N.-H. (1979) Proc. Natl. Acad. Sci. USA 76, 111–115.
32 Eskins, K., McCarthy, S.A. and Duysen, M. (1986) Physiol. Plant. 67, 242–246.
33 Laskey, R.A. and Mills, A.D. (1975) Eur. J. Biochem. 56, 335–341.
34 Bonner, W.M. and Laskey, R.A. (1974) Eur. J. Biochem. 46, 83–88.
35 Tobin, H., Staehelin, T. and Gordon, J. (1979) Proc. Natl. Acad. Sci. USA 76, 4350–4354.
36 Groome, N.J. (1980) Clin. Chem. Clin. Biochem. 18, 345–349.
37 Klotz, I.M. and Hunston, D.L. (1971) Biochemistry 10, 3065–3069.
38 Dennenberg, R.J., Jursinic, P.A. and McCarthy, S.A. (1986) Biochim. Biophys. Acta 852, 222–233.
39 Duysens, L.N.M. and Sweers, H.E. (1963) In Studies in Microalgae and Photosynthetic Bacteria (Japan Society of Plant Physiology, eds.) pp. 353–372. Tokyo, University of Tokyo Press.
40 Joliot, P., Joliot, A., Bouges, B. and Barbieri, G. (1971) Photochem. Photobiol. 14, 287–305.
41 Mauzerall, D. (1972) Proc. Natl. Acad. Sci. USA 69, 1358–1362.
42 Bennoun, P. (1970) Biochim. Biophys. Acta 216, 357–363.
43 Mohanty, P., Mar, T. and Govindjee (1971) Biochim. Biophys. Acta 253, 213–221.
44 Robinson, H.H. and Crofts, A. (1983) FEBS Lett. 153, 221–226.
45 Hideg, E. and Demeter, S. (1985) Z. Naturforsch. 40C, 827–831.
46 Cheniae, G.M. and Martin, I.F. (1971) Plant Physiol. 47, 568–575.
47 Lavergne, J. (1982) Biochim. Biophys. Acta 679, 12–18.
48 Gardner, G. (1981) Science 211, 937–940.
49 Mullet, J.E. and Arntzen, C.J. (1981) Biochim. Biophys. Acta 635, 236–248.
50 Metz, J.G., Pakrasi, H.B., Seibert, M. and Arntzen, C.J. (1986) FEBS Lett. 205, 269–274.
51 Odom, W.R. and Bricker, T.M. (1990) Photosynthetica 24, 46–55.
52 Reisfeld, A., Mattoo, A.K. and Edelman, M. (1982) Eur. J. Biochem. 124, 125–129.
53 Stemler, A. and Murphy, J. (1984) Plant Physiol. 76, 179–182.
54 Mattoo, A., Pick, U., Hoffman-Falk, H. and Edelstein, M. (1981) Proc. Natl. Acad. Sci. USA 78, 1572–1576.
55 Ohad, I., Kyle, D. and Arntzen, C.J. (1984) J. Cell Biol. 99, 481–485.
56 Wettern, M. (1986) Plant Sci. 43, 173–177.
57 Eckenswiller, L.C. and Greenberg, B.M. (1989) Plant Physiol. Suppl. 89, 944.
58 Greenberg, B.M., Gaba, V., Mattoo, A.K. and Edelman, M. (1987) EMBO J. 6, 2865–2869.
59 Jursinic, P. and Stemler, A. (1988) Photosyn. Res. 15, 41–56.
60 Jursinic, P. and Stemler, A. (1982) Biochim. Biophys. Acta 681, 419–428.
61 Chow, W.S. and Hope, A.B. (1987) Aust. J. Plant Physiol. 14, 21–28.
62 Rochaix, J.D., Dron, M., Rahire, M. and Malnoé, P. (1984) Plant Mol. Biol. 3, 363–370.